Mon. Not. R. Astron. Soc. **361,** 965–970 (2005) doi:10.1111/j.1365-2966.2005.09221.x

High-energy afterglow emission from giant flares of soft gamma-ray repeaters: the case of the 2004 December 27 event from SGR 1806–20

Y. Z. Fan,[1,2,3⋆] Bing Zhang[3⋆] and D. M. Wei[1,2⋆]

[1]*Purple Mountain Observatory, Chinese Academy of Science, Nanjing 210008, China*
[2]*National Astronomical Observatories, Chinese Academy of Sciences, Beijing 100012, China*
[3]*Department of Physics, University of Nevada, Las Vegas, NV 89154, USA*

Accepted 2005 May 23. Received 2005 May 6

ABSTRACT

We discuss the high-energy afterglow emission (including high-energy photons, neutrinos and cosmic rays) following the 2004 December 27 giant flare from the soft gamma-ray repeater (SGR) 1806−20. If the initial outflow is relativistic with a bulk Lorentz factor $\Gamma_0 \sim$ tens, the high-energy tail of the synchrotron emission from electrons in the forward shock region gives rise to a prominent sub-GeV emission, if the electron spectrum is hard enough and if the initial Lorentz factor is high enough. This signal could serve as a diagnosis of the initial Lorentz factor of the giant flare outflow. This component is potentially detectable by the *Gamma-Ray Large Area Telescope* (*GLAST*) if a similar giant flare occurs in the *GLAST* era. With the available 10-MeV data, we constrain that $\Gamma_0 < 50$ if the electron distribution is a single power law. For a broken power-law distribution of electrons, a higher Γ_0 is allowed. At energies higher than 1 GeV, the flux is lower because of a high-energy cut-off of the synchrotron emission component. The synchrotron self-Compton emission component and the inverse Compton scattering component off the photons in the giant flare oscillation tail are also considered, but they are found not significant given a moderate Γ_0 (e.g. $\leqslant 10$). The forward shock also accelerates cosmic rays to the maximum energy 10^{17} eV, and generates neutrinos with a typical energy 10^{14} eV through photomeson interaction with the X-ray tail photons. However, they are too weak to be detectable.

Key words: acceleration of particles – elementary particles – hydrodynamics – stars: neutron – stars: winds, outflows – gamma-rays: bursts.

1 INTRODUCTION

The soft gamma-ray repeater (SGR) 1806−20 lies in the Galactic plane, at a distance of about $D_{\rm L} \approx 15.1$ kpc (Corbel & Eikenberry 2004; cf. Cameron et al. 2005). A giant flare originated from it on 2004 December 27, and is the brightest extrasolar transient event ever recorded (e.g. Hurley et al. 2005; Palmer et al. 2005). Radio follow-ups have resulted in detections of its afterglow (e.g. Cameron et al. 2005; Gaensler et al. 2005). Thanks to its brightness, an amazing variety of data, including the source size, shape, polarization and flux at multifrequencies as a function of time, has been collected (e.g. Cameron et al. 2005; Gaensler et al. 2005; Gelfand et al. 2005). Even so, our understanding of the outflow is still in dispute. For example, the earliest afterglow data obtained so far is about 7 d after the giant flare. At this epoch, even an initially relativistic outflow has been decelerated to the Newtonian phase by the interstellar medium (ISM). As a result, whether the outflow is relativistic initially (e.g. Dai et al. 2005; Wang et al. 2005) or not (e.g. Gelfand et al. 2005; Granot et al. 2005) is uncertain. In principle, similar to the gamma-ray burst (GRB) case (e.g. Krolik & Pier 1991), if the spectrum of the giant flare is non-thermal, a lower bound of the initial Lorentz factor $\Gamma_0 \sim$ tens can be derived from the so-called 'compactness argument' (e.g. Huang, Dai & Lu 1998; Thompson & Duncan 2001; Ioka et al. 2005; Nakar, Piran & Sari 2005). Observationally, the giant flare spectrum may be thermal (Hurley et al. 2005) or non-thermal (Palmer et al. 2005), so that Γ_0 could not be constrained well.

In order to understand the dynamical evolution of the outflow better, early multiwavelength (including optical and hard gamma-ray band) observations are greatly needed. The early optical emission has already been calculated in Cheng & Wang (2003) and Wang et al. (2005). In this work, we focus on the high-energy afterglow emission, including sub-GeV photons (see Section 2), high-energy neutrinos and cosmic rays (see Section 3). High-energy neutrinos from magnetars in the quiescent state have been discussed by Zhang et al. (2003). Assuming the internal shock mechanism, the neutrino,

⋆E-mail: yzfan@pmo.ac.cn (YZF); bzhang@physics.unlv.edu (BZ); dmwei@pmo.ac.cn (DMW)

cosmic ray and TeV photon emission accompanying the prompt giant flare have been discussed recently (Asano, Yamazaki & Sugiyama 2005; Halzen, Landsman & Montaruli 2005; Ioka et al. 2005).

2 HIGH-ENERGY PHOTON EMISSION

We first take $\Gamma_0 = 10$ as the typical Lorentz factor of the flow to perform sample calculations. The effect of varying Γ_0 will be discussed later. The isotropic energy of the outflow is taken as $E_{\rm iso} \sim 10^{46}$ erg. In the following analytical discussion, we assume that the shocked electrons distributes as a single power law $\mathrm{d}n/\mathrm{d}\gamma_{\rm e} \propto \gamma_{\rm e}^{-\rm p}$ for $\gamma_{\rm m} < \gamma_{\rm e} < \gamma_{\rm M}$, where $p \sim 2.5$, $\gamma_{\rm M} \sim 10^8\ B'^{-1/2}$ (B' is the shock-generated magnetic field strength; see equation 4). Wang et al. (2005) find that a broken power-law distribution of electrons, i.e. $\mathrm{d}n/\mathrm{d}\gamma_{\rm e} \propto \gamma_{\rm e}^{-\rm p_1}$ for $\gamma_{\rm m} < \gamma_{\rm e} < \gamma_{\rm b}$ and $\mathrm{d}n/\mathrm{d}\gamma_{\rm e} \propto \gamma_{\rm e}^{-\rm p_2}$ for $\gamma_{\rm b} < \gamma_{\rm e} < \gamma_{\rm M}$, is required to interpret the chromatic radio afterglow light curve steepening around day 9. We therefore also include such a possibility in the numerical calculations (see Section 2.3).

With the standard parameters, the relativistic outflow is decelerated by the ISM in a time-scale

$$t_{\rm dec} \approx 300\ {\rm s}\ E_{\rm iso,46}^{1/3} n_0^{-1/3} \Gamma_{0,1}^{-8/3}, \tag{1}$$

after which the ejecta moves with the Lorentz factor (for $\Gamma > 1/\theta_{\rm j}$)

$$\Gamma \approx 5.8 E_{\rm iso,46}^{1/8} n_0^{-1/8} t_{\rm obs,3}^{-3/8}, \tag{2}$$

where n is the number density of the ISM and $t_{\rm obs}$ is the observer time in unit of seconds. Throughout the paper, we adopt the convention $Q_{\rm a} = Q/10^{\rm a}$ using cgs units.

As usual, we assume $\epsilon_{\rm e}$ and ϵ_B as the shock energy equipartition parameters for the shock accelerated electrons and the magnetic fields, respectively. The minimum electron Lorentz factor reads

$$\gamma_{\rm m} \approx 184 C_{\rm p} \epsilon_{\rm e,-0.5} (\Gamma - 1). \tag{3}$$

where $C_{\rm p} = 3(p-2)/(p-1)$. The strength of shock generated magnetic fields can be estimated as

$$B' \approx 3.9 \times 10^{-2}\ {\rm G}\ \epsilon_{B,-2}^{1/2} n_0^{1/2} [\Gamma(\Gamma-1)]^{1/2}. \tag{4}$$

Throughout the paper, the superscript $'$ represents the parameter measured in the comoving frame of the ejecta.

2.1 Inverse Compton radiation

A soft thermal X-ray tail emission modulated by the magnetar period is typically detected after a giant flare hard spike. For the December 27 event from SGR 1806−20, such a tail lasts for $T_{\rm tail} \sim 300$ with a typical photon energy $\epsilon_{\rm X} \sim 30$ keV (e.g. Mazets et al. 2005) and a luminosity $L_{\rm X} \sim 2 \times 10^{43}\ {\rm erg\ s^{-1}}\ (t_{\rm obs}/50\ {\rm s})^{-1}$. For $t_{\rm obs} < T_{\rm tail}$, besides the synchrotron and synchrotron-self-Compton (SSC) cooling processes (see Section 2.2 for detail), the electrons in the shocked region are also cooled by inverse Compton (IC) scattering off these X-ray tail photons.

Because $T_{\rm tail}$ is comparable to $t_{\rm dec}$, the ejecta has not decelerated significantly, i.e. $\Gamma \sim \Gamma_0$. In the comoving frame of the ejecta, the energy density of the X-ray tail reads

$$U'_{\rm X} \approx \frac{L_{\rm X}}{4\pi R^2 c \Gamma^2} \approx 0.027\ {\rm erg\ cm^{-3}}\ L_{\rm X,42} R_{15}^{-2} \Gamma_1^{-2}, \tag{5}$$

where R is the radial distance of the forward shock front from the central source. On the other hand, the magnetic energy density generated in the forward shock front reads

$$U'_B \approx 6 \times 10^{-3}\ {\rm erg\ cm^{-3}}\ \epsilon_{B,-2} \Gamma_1^2 n_0. \tag{6}$$

In the rest frame of the shocked electrons with a random Lorentz factor $\gamma_{\rm e}$, the energy of the thermal tail $\gamma_{\rm e}\epsilon_{\rm X}/\Gamma$ is much larger than $m_{\rm e}c^2$, so that the Klein–Nishina correction is important. For convenience, we define $x \equiv \gamma_{\rm e}\epsilon_{\rm X}/\Gamma m_{\rm e}c^2 \simeq \gamma_{\rm e}/17\Gamma$. In the Klein–Nishina limit, $\sigma_{\rm IC} = A(x)\sigma_{\rm T}$, where

$$A(x) \equiv \frac{3}{4}\left\{\frac{1+x}{x^3}\left[\frac{2x(1+x)}{1+2x} - \ln(1+2x)\right] + \frac{1}{2x}\ln(1+2x) - \frac{1+3x}{(1+2x)^2}\right\},$$

with the asymptotic limits

$$A(x) \approx 1 - 2x + \frac{26x^2}{5} \qquad \text{for } x \ll 1,$$

and

$$A(x) \approx \frac{3}{8} x^{-1}\left(\ln 2x + \frac{1}{2}\right) \qquad \text{for } x \gg 1$$

(e.g. Rybicki & Lightman 1979).

For illustration, we take $t_{\rm obs} = T_{\rm tail}$, at which $R \approx 2\Gamma^2 c T_{\rm tail} \approx 1.8 \times 10^{15}\ {\rm cm}\ \Gamma_1^2 T_{\rm tail,2.5}$. For $\gamma_{\rm e} = \gamma_{\rm m}$, we have $x = 10.8$, $A(x = 10.8) \approx 0.1$. The IC scattering is therefore in the extreme Klein–Nishina limit, and the typical IC photon energy can be well approximated by

$$\begin{aligned} h\nu_{\rm m}^{\rm IC} &\approx h\Gamma\gamma_{\rm m} m_{\rm e} c^2 \approx \epsilon_{\rm e}[(p-2)/(p-1)](\Gamma-1)\Gamma m_{\rm p} c^2 \\ &\approx 9\ {\rm GeV}\ C_{\rm p} \epsilon_{\rm e,-0.5} \Gamma_1^2. \end{aligned} \tag{7}$$

The IC optical depth is

$$\tau \sim A(10.8)\sigma_{\rm T} n R/3 \sim 4 \times 10^{-11} n_0 R_{15.26}, \tag{8}$$

so that the 10-GeV photon luminosity can be estimated by

$$\begin{aligned} L_{10\,{\rm GeV}} &\sim \tau (L_{\rm X}/\epsilon_{\rm X})(h\nu_{\rm m}^{\rm IC}) \\ &\sim 4.3 \times 10^{37}\ {\rm erg\ s^{-1}}\ n_0 R_{15.26} t_{\rm obs,2.5}^{-1}, \end{aligned} \tag{9}$$

where h is the Planck constant. For $T_{\rm tail} \leqslant t_{\rm dec}$, $\Gamma \sim \Gamma_0$, $R \propto t_{\rm obs}$ we have $L_{10\,{\rm GeV}} \propto R t_{\rm obs}^{-1} \propto t_{\rm obs}^0$. We can then estimate the total number of the photons detectable by the *Gamma-Ray Large Area Telescope* (*GLAST*; see http://glast.gsfc.nasa.gov/) in construction

$$\begin{aligned} N_{\rm tot}(10\,{\rm GeV}) &\sim \left[\frac{A_{GLAST}}{4\pi D_{\rm L}^2}\int_0^{T_{\rm tail}} L_{10\,{\rm GeV}}\,\mathrm{d}t_{\rm obs}\right]/10\,{\rm GeV} \\ &\sim 0.03\ T_{\rm tail,2.5} n_0 (D_{\rm L}/15.1\,{\rm kpc})^{-2}, \end{aligned} \tag{10}$$

where $A_{GLAST} \approx 8000\ {\rm cm}^2$ is the effective area of the *GLAST*. Because usually at least five photons are needed to claim a detection (e.g. Zhang & Mészáros 2001 and references therein), the above predicted $N_{\rm tot}$ is well below the threshold of *GLAST*. This component is undetectable for an energetic giant flare similar to the recent one even for a much closer SGR, for example, SGR 1900+14.

The thermal tail photons would be also scattered by the electrons accelerated by the reverse shock. The reverse shock is expected subrelativistic. At $t_{\rm dec}$, $\gamma_{34} \sim 1.2$, where γ_{34} is the Lorentz factor of shocked region relative to initial unshocked outflow. Therefore, for the electrons accelerated by the reverse shock, we have $\gamma_{\rm m}^{\rm r} = \epsilon_{\rm e}\,[(p-2)/(p-1)]\,(m_{\rm p}/m_{\rm e})\,(\gamma_{34}-1) \sim 37$ by assuming the same parameters as in the forward shock region. Therefore, $\epsilon_{\rm x}$ will be

scattered to an energy $\sim \gamma_{\rm m}^{\rm r2}\epsilon_{\rm x} \sim 30$ MeV. According to equations (9) and (10), the detected number of photons essentially depends on the IC optical depth τ and is independent of the typical energy of the photons. We can then estimate the total number of IC photons from the reverse shock region by comparing that in the forward shock region. First, the IC is now in the Thomson regime, i.e. $\sigma_{\rm IC} \simeq \sigma_{\rm T}$. Secondly, the total number of electrons contained in the reverse shock region is about Γ_0 times that in the forward shock region. The expected total number of the 30 MeV photons is therefore

$$N_{\rm tot}(30\,{\rm MeV}) \sim \frac{\Gamma_0}{A(x=10.8)} N_{\rm tot}(10\,{\rm GeV}) \sim 3. \quad (11)$$

The actual value should be smaller because the time-scale of having a strong reverse shock could be shorter than $T_{\rm tail}$. Although this $\sim$30 MeV reverse shock component is more prominent than the $\sim$10 GeV forward shock component, it is undetectable by *GLAST*.

2.2 Synchrotron and synchrotron-self-Compton radiation

For the forward shock emission, the cooling frequency $\nu_{\rm c}$, the typical synchrotron frequency $\nu_{\rm m}$ and the maximum spectral flux $F_{\nu,\rm max}$ read (e.g. Cheng & Wang 2003; Wang et al. 2005)

$$\nu_{\rm c} = 3.1\times10^{19}\,{\rm Hz}\,E_{\rm iso,46}^{-1/2}\epsilon_{B,-2}^{-3/2}n_0^{-1}t_{\rm obs,3}^{-1/2}(1+Y)^{-2}, \quad (12)$$

$$\nu_{\rm m} = 2.4\times10^{12}\,{\rm Hz}\,C_{\rm p}^2E_{\rm iso,46}^{1/2}\epsilon_{B,-2}^{1/2}\epsilon_{\rm e,-0.5}^{2}t_{\rm obs,3}^{-(3/2)}, \quad (13)$$

$$F_{\nu,\rm max} = 474\,{\rm Jy}\,E_{\rm iso,46}\epsilon_{B,-2}^{1/2}n_0^{1/2}\left(\frac{D_{\rm L}}{15.1\,{\rm kpc}}\right)^{-2}. \quad (14)$$

Here, Y is the IC parameter, which can be estimated by $Y \simeq [-1+\sqrt{1+4x\epsilon_{\rm e}/\epsilon_B}]/2$ (e.g. Sari & Esin 2001), where $x = \min[1, 2.67(\gamma_{\rm m}/\gamma_{\rm c})^{(p-2)}]$ is the radiation coefficient of the shocked electrons (see equation A8 of Fan, Zhang & Wei 2005a), and $\gamma_{\rm c}$ is the electron cooling Lorentz factor

$$\gamma_{\rm c} \approx \frac{7.7\times10^8}{(1+Y)}\frac{1}{\Gamma B'^2 t_{\rm obs}}. \quad (15)$$

Notice that only the SSC is considered. The IC component discussed in Section 2.1 is in the extreme Klein–Nishina regime at $\gamma_{\rm c}$, giving a very small contribution to the Y parameter. So it is neglected. The resulting flux at a typical energy $h\nu_{\rm obs} = 0.1$ GeV can then be estimated as

$$\begin{aligned} F_{\nu_{\rm obs}} &= F_{\nu,\rm max}\nu_{\rm c}^{1/2}\nu_{\rm m}^{(p-1)/2}\nu_{\rm obs}^{-p/2} \\ &= 1.2\times10^{-6}\,{\rm erg\,cm^{-2}GeV^{-1}}\epsilon_{\rm e,-0.5}^{p-1}\epsilon_{B,-2}^{[(p-2)/4]} \\ &\quad\times E_{46}^{[(p+2)/4]}C_{\rm p}^{(p-1)}\left(\frac{D_{\rm L}}{15.1\,{\rm kpc}}\right)^{-2}t_{\rm obs,3}^{[(2-3p)/4]} \\ &\quad\times(1+Y)^{-1}\left(\frac{h\nu_{\rm obs}}{0.1\,{\rm GeV}}\right)^{[-(p-1)/2]}. \end{aligned} \quad (16)$$

For typical parameters, Y is of the order of 1, so the flux is much higher than that of typical GRBs, so that this component can be detected by *GLAST*. Notice that there exists an upper limit on the synchrotron radiation energy

$$h\nu_{\rm M} \sim 2.8\times10^6 h\gamma_{\rm M}^2\Gamma B' \sim 1.2\,{\rm GeV}\,\Gamma_1, \quad (17)$$

above which a sharp cut-off is expected.

Because the outflow is only mildly relativistic, the collimation effect is important in calculating the late light curves. Following Yamazaki et al. (2005), we adopt a half-opening angle of the collimated outflow $\theta_{\rm j} \approx 0.3$. This leads to a geometry corrected energy $\approx E_{\rm iso}\,\theta_{\rm j}^2/4 \approx 2.2\times10^{44}$ erg $E_{\rm iso,46}\,(\theta_{\rm j}/0.3)^2$, which matches that derived from the radio afterglow modelling (e.g. Wang et al. 2005). The above analytical calculations are only valid for $\Gamma > 1/\theta_{\rm j}$. For $\Gamma < 1/\theta_{\rm j}$, the jet sideways expansion effect is important. A rough estimate gives $\Gamma(J_{\rm s}) \propto t_{\rm obs}^{-1/2}$, $F_{\nu,\rm max}(J_{\rm s}) \propto t_{\rm obs}^{-1}$, $\nu_{\rm c}(J_{\rm s}) \propto$ const. and $\nu_{\rm m}(J_{\rm s}) \propto t_{\rm obs}^{-2}$ (e.g. Rhoads 1999), where $J_{\rm s}$ represents the jet with important sideways expansion. Defining the 'jet break' time $t_{\rm j} \approx 4500$ s $\Gamma_{0,1}^{-8/3}E_{\rm iso,46}^{1/3}n_0^{-1/3}$, for $t_{\rm obs} > t_{\rm j}$, the flux could be estimated as $F_{\nu_{\rm obs}} \simeq 1.8\times10^{-7}\,{\rm erg\,cm^{-2}\,GeV^{-1}}\,(t_{\rm obs}/t_{\rm j})^{-p}(1+Y)^{-1}(h\nu_{\rm obs}/0.1\,{\rm GeV})^{-p/2}$. Because the typical Lorentz factor is small ($\sim$10), the above analytical treatment may not be a good approximation, and more detailed numerical calculations are needed (see Section 2.3). The SSC luminosity ($L_{\rm SSC}$) could be estimated through the Y parameter, i.e. $Y = L_{\rm SSC}/L_{\rm syn}$. This results in the maximum SSC spectral flux (for $t_{\rm dec} < t_{\rm obs} < t_{\rm j}$)

$$F_{\nu_{\rm max}^{\rm SSC}} \approx Y\gamma_{\rm c}^{p-3}\gamma_{\rm m}^{1-p}F_{\nu,\rm max} \quad (18)$$

where $\nu_{\rm m}^{\rm SSC}$ is the typical SSC frequency

$$\begin{aligned} \nu_{\rm m}^{\rm SSC} &\approx \gamma_{\rm m}^2\nu_{\rm m} \approx 1.9\times10^{18}\,{\rm Hz}\,C_{\rm p}^4\epsilon_{\rm e,-0.3}^4 \\ &\quad \epsilon_{B,-2}^{1/2}n_0^{-1/4}E_{\rm iso,46}^{3/4}t_{\rm obs,3}^{-9/4}. \end{aligned} \quad (19)$$

The resulting flux at $h\nu_{\rm obs} = 0.1$ GeV reads

$$\begin{aligned} F_{\nu_{\rm obs}} &= F_{\nu_{\rm max}^{\rm SSC}}\left(\nu_{\rm obs}/\nu_{\rm m}^{\rm SSC}\right)^{-(p-1)/2} \\ &= 2.2\times10^{-8}\,{\rm erg\,cm^{-2}\,GeV^{-1}}\,Y(1+Y)^{p-3}C_{\rm p}^{p-1} \\ &\quad\times\epsilon_{\rm e,-0.5}^{p-1}\epsilon_{B,-2}^{(13-3p)/4}n_0^{(13-3p)/8}E_{\rm iso,46}^{(15-p)/8}t_{\rm obs,3}^{(3-5p)/8} \\ &\quad\times(D_{\rm L}/15.1\,{\rm kpc})^{-2}(h\nu_{\rm obs}/0.1\,{\rm GeV})^{-(p-1)/2}. \end{aligned} \quad (20)$$

For $h\nu_{\rm obs} \leqslant 0.1$ GeV, this radiation component is much weaker than the synchrotron component. Beyond the synchrotron cut-off at $h\nu_{\rm obs} \sim 1$ GeV, the SSC component dominates, but it is well below the *GLAST* threshold.

2.3 Numerical results

Similar to Huang et al. (2000) and Cheng & Wang (2003), we have calculated the dynamical evolution of the ejecta (see Fig. 1) and the accompanying high-energy photon emission (see Fig. 2) numerically.

As shown in Fig. 1, the jet half-opening angle increases with time rapidly. With sideways expansion, the evolution of the jet half-opening angle could be written as (e.g. Huang et al. 2000) $\mathrm{d}\theta/\mathrm{d}t_{\rm obs} = c_{\rm s}(\Gamma+\sqrt{\Gamma^2-1})/R$, where $c_{\rm s} \approx \sqrt{(4\Gamma+3)(\Gamma^2-1)/[3\Gamma(4\Gamma^2-1)]}c$ is the local sound speed. For $\Gamma \gg 1$, this could be approximated as $\mathrm{d}\theta/\mathrm{d}t_{\rm obs} \approx 1.2/(2\Gamma t_{\rm obs})$. It is apparent that the sideways expansion of the jet is very important from the very beginning of the dynamical evolution if the initial Lorentz factor is as small as 10. As a result, there is no jet break in the $(\Gamma-1)$ light curve (Fig. 1) or the energy flux light curve (Fig. 2). This is different from the case of ultrarelativistic GRB outflows, in which the sideways expansion is important only at later times. One conclusion drawn from Fig. 1 is that the ejecta accounting for the radio afterglow is nearly isotropic, which matches the observations well (e.g. Cameron et al. 2005; Gaensler et al. 2005).

According to Fig. 2 where $\Gamma_0 = 10$ is adopted, we can see that the predicted energy flux in the 0.05–0.15 GeV band is above the *GLAST* sensitivity (thick dashed line), especially when a single power-law electron energy distribution (thin dashed line) is adopted. If the electron distribution is a broken power law (solid line), the detectability

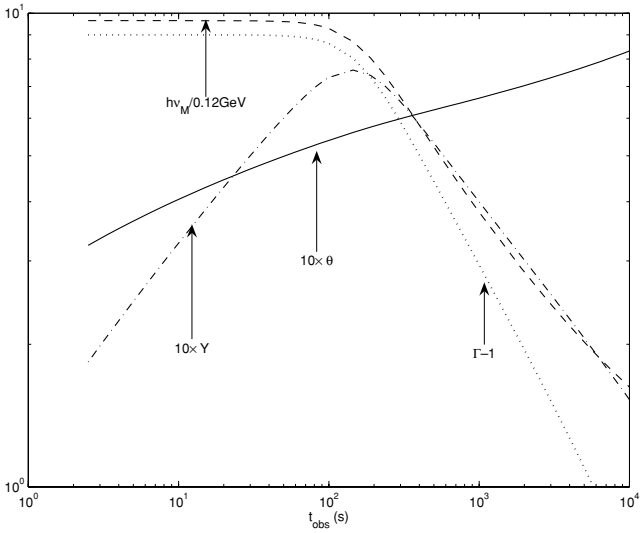

Figure 1. Dynamical evolution of the ejecta. The dotted line represents $\Gamma - 1$, the solid line represents θ (multiplied by 10), the dash-dotted line represents the SSC parameter Y (multiplied by 10) and the dashed line represents the cut-off energy of synchrotron radiation $h\nu_{\rm M}$ (normalized to 0.12 GeV), all as functions of time. The following initial parameters are adopted: $E_{\rm iso} = 10^{46}$ erg, $\theta_{\rm j} = 0.3$, $\Gamma_0 = 10$, $n = 1$ cm^{-3}, $\epsilon_{\rm e} = 0.3$, $\epsilon_B = 0.01$ and $p = 2.5$. The starting point of the calculation is taken as $R_0 = 10^{13}$ cm.

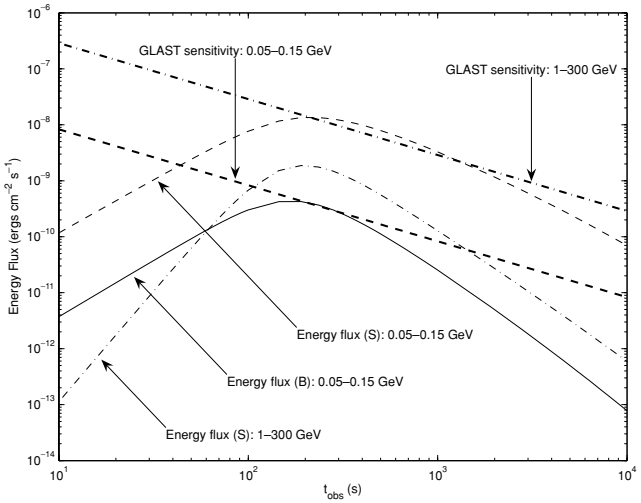

Figure 2. Predicted photon energy fluxes compared with the *GLAST* flux sensitivity. The thin dashed line and the solid line represent the flux in the energy range 0.05–0.15 GeV for different electron energy distributions, where 'S' denotes single power law and 'B' denotes broken power law. Only the synchrotron component is calculated because the SSC component is much dimmer. The thin dash-dotted line represents the flux in the 1–300 GeV energy band. Only the SSC component is calculated because this is above the synchrotron cut-off energy. The thick dashed line and the thick dash-dotted line represent the *GLAST* threshold in the energy ranges 0.05–0.15 and 1–300 GeV, respectively. The *GLAST* threshold is defined by requiring that during the integration time-scale $\sim t_{\rm obs}$ at least five photons are collected. For the thin dashed and dash-dotted lines, the same parameters as those in Fig. 1 are taken. For the solid line, the parameters are the same as those taken in Fig. 1 except that $p_1 = 2.2$, $p_2 = 3.2$ (rather than p), and $\gamma_b/\gamma_m = 120$ are adopted.

by *GLAST* is only marginal. In the energy band above 1 GeV, the predicted SSC energy flux (thin dash-dotted line) is always below the *GLAST* sensitivity (thick dash-dotted line), so that it is undetectable.

In Fig. 3, we investigate the dependence of the predicted 0.05–0.15 GeV energy flux (only the synchrotron radiation component is taken into account) on Γ_0. The general trend is that a higher Γ_0 leads to a stronger sub-GeV emission. For $\Gamma_0 \sim$ tens, regardless of the distribution of the shocked electrons (single power law or broken power law), the predicted fluxes are all above the *GLAST*. For $\Gamma_0 \sim$ a few, only the single power law distribution model can yield to marginally observable 0.05–0.15 GeV photon emission.

In principle, a measurement of the sub-GeV flux in the *GLAST* era could serve as a diagnosis of the initial Lorentz factor of the outflow. For SGR 1806-60, available data already give interesting constraints. According to Mazets et al. (2005), the time-averaged energy flux in the $\epsilon_\gamma \sim 10$ MeV band could be estimated as $\epsilon_\gamma^2 {\rm d}N/{\rm d}\epsilon_\gamma \sim 1.6 \times 10^{-6}$ erg cm^{-2} s^{-1}, where ${\rm d}N/{\rm d}\epsilon_\gamma \sim 10^{-5}$ photons cm^{-2} s^{-1} keV^{-1} is the photon number spectrum of the tail emission at 10 MeV. Compared with our numerical results presented in Fig. 3, the single power-law distribution model with $\Gamma_0 = 50$ is already above the observed level.[1] A Lorentz factor $\Gamma_0 \geqslant 50$ is allowed only when a broken power-law distribution of the electrons is assumed.

3 COSMIC RAYS AND NEUTRINOS

Below we estimate the maximum proton energy ($\epsilon_{\rm p}^{\rm M}$) accelerated by the forward shock. For simplicity, we only discuss $t_{\rm dec} < t_{\rm obs} < t_{\rm j}$.

[1] Our calculated energy flux is in the $\epsilon_\gamma = 50$–150 MeV band. However, because $\nu_{\rm obs} F_{\nu_{\rm obs}} \propto \nu_{\rm obs}^{(2-p)/2}$ very weakly depends on $\nu_{\rm obs}$, the results could approximately apply to the 10-MeV band as well.

In general, $\epsilon_{\rm p}^{\rm M} = \min[\epsilon_{\rm p}^{\rm M}(1), \epsilon_{\rm p}^{\rm M}(2), \epsilon_{\rm p}^{\rm M}(3)]$ satisfies three constraints (see also Fan, Zhang & Wei 2005b).

(i) The comoving shock acceleration time $t'_{\rm a} \sim \epsilon_{\rm p}/\Gamma eB'c$ should be smaller than the comoving wind expansion time $t'_{\rm d} \sim R/\Gamma c$, which yields $\epsilon_{\rm p}^{\rm M}(1) \sim eB'\,R$. The numerical value reads

$$\epsilon_{\rm p}^{\rm M}(1) \simeq 2.4 \times 10^{17}\ {\rm eV}\ \epsilon_{B,-2}^{1/2} n_0^{1/8} E_{\rm iso,46}^{3/8} t_{\rm obs,3}^{-1/8}. \quad (21)$$

(ii) The comoving proton synchrotron cooling time-scale $t'_{\rm cool} = (6\pi m_{\rm p}^4 c^3/\sigma_{\rm T} m_{\rm e}^2)\Gamma\epsilon_{\rm p}^{-1} B'^{-2}$ should be longer than the comoving acceleration time-scale $t'_{\rm a}$, which results in

$$\epsilon_{\rm p}^{\rm M}(2) \simeq 2.6 \times 10^{21}\ {\rm eV}\ \epsilon_{B,-2}^{-1/4} E_{\rm iso,46}^{1/16} n_0^{-5/16} t_{\rm obs,3}^{-3/16}. \quad (22)$$

(iii) The comoving proton cooling time-scale due to photomeson interaction should also be longer than the comoving acceleration time-scale $t'_{\rm a}$. However, from equation (13), the typical frequency of the forward shock emission is too low to provide the target photons for photomeson interactions at the Δ resonance, so the effect of photomeson interaction is too small to change the proton cooling process.

Therefore, one has $\epsilon_{\rm p}^{\rm M} = \epsilon_{\rm p}^{\rm M}\,(1) \sim 2.4 \times 10^{17}$eV. The source location of SGR 1806−20 is about 10° from the Galactic Centre. In the region near the Galactic Centre the magnetic field structure is poorly constrained. The time delay due to the interstellar random

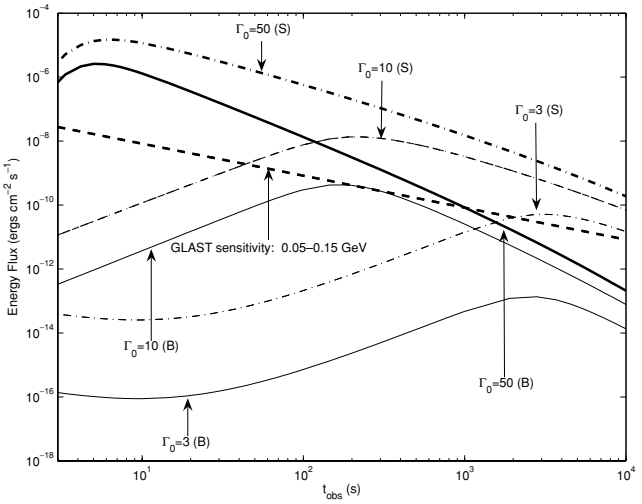

Figure 3. The dependence of predicted 0.05–0.15 GeV photon energy flux on the initial Lorentz factor Γ_0, whose actual values have been marked in the figure. Both single power-law ('S') and broken power-law ('B') distributions of the electrons are calculated. The thick dashed line represents the *GLAST* sensitivity in the energy range 0.05–0.15 GeV. Except for Γ_0, the other parameters are the same as those in Fig. 2.

magnetic field can be approximated as (e.g. Asano et al. 2005)

$$T_{\rm delay} \simeq (eB_{\rm G}D_{\rm L}/\epsilon_{\rm CR})^2(l/c), \quad (23)$$

where $B_{\rm G} \sim 10^{-6}$ G is the average magnetic field strength in the Galaxy, $\epsilon_{\rm CR}$ is the typical cosmic ray energy, and $l \sim$ 10–100 pc is the correlation length of the magnetic field (e.g. Asano et al. 2005). We then obtain $T_{\rm delay} \approx 6 \times 10^5$ yr $B^2_{\rm G,-6}(D_{\rm L}/15.1\ {\rm kpc})^2(l/10\ {\rm pc})\epsilon^{-2}_{\rm CR,17}$. As a result, these cosmic rays become a part of the cosmic ray background.

As shown in equation (13), the typical frequency of the forward shock emission is too low to provide the target photons for the photomeson interaction at the Δ-resonance. The only interesting source of the neutrino emission is then the photomeson interaction during the early epoch when the X-ray tail overlaps with the shocked region. In the comoving frame of the ejecta, the thermal tail photons with energy $\approx \epsilon_{\rm X}/\Gamma$ interact with the protons with energy

$$\epsilon_{\rm p} \sim 0.3\Gamma^2\,{\rm GeV}^2/\epsilon_{\rm X} \simeq 10^{16}\,{\rm eV}\,\Gamma_1^2(\epsilon_{\rm X}/30\,{\rm keV})^{-1}. \quad (24)$$

These protons lose ∼20 per cent of their energy at each $p\gamma$ interaction, dominated by the Δ-resonance. Approximately, half of the pions are charged and decay into high-energy neutrinos $\pi^+ \rightarrow \mu^+ + \nu_\mu \rightarrow {\rm e}^+ + \nu_{\rm e} + \bar{\nu}_\mu + \nu_\mu$, with the energy distributed roughly equally among the decay products (e.g. Ioka et al. 2005). Therefore the neutrino energy is ∼5 per cent of the proton energy, i.e.

$$\epsilon_\nu \sim 5 \times 10^{14}\,{\rm eV}\,\Gamma_1^2(\epsilon_{\rm X}/30\,{\rm keV})^{-1}. \quad (25)$$

The comoving number density of the thermal photons at the radius $R \sim 10^{15}$ cm is

$$n_{\rm X} \approx \Gamma U'_{\rm X}/\epsilon_{\rm X} \approx 5.5 \times 10^7 L_{\rm X,43}R_{15}^{-2}\Gamma_1^{-1}(\epsilon_{\rm X}/30\,{\rm keV})^{-1}. \quad (26)$$

The fraction of the energy converted to pions can be estimated by the number of the p–γ interactions occurring within the shock with the characteristic width $\Delta R \sim R/\Gamma$, i.e.

$$f_\pi \simeq 0.2 n_{\rm X}\sigma_\Delta R/\Gamma \simeq 5.5 \times 10^{-7} L_{\rm X,43}R_{15}^{-1}\Gamma_1^{-2}(\epsilon_{\rm X}/30\,{\rm keV})^{-1}, \quad (27)$$

where $\sigma_\Delta \sim 5 \times 10^{-28}$ cm^2 is the cross-section of the Δ-resonance.

For a neutrino detector with an area $A_{\rm det} \sim 10^{10}$ cm^2, the expected event number is

$$N_\nu \sim P_{\nu\rightarrow\mu} f_\pi A_{\rm det} E_{\rm iso}/\left(32\pi D_{\rm L}^2\epsilon_\nu\right) \sim 7 \times 10^{-5}, \quad (28)$$

where $P_{\nu\rightarrow\mu} \simeq 3.5 \times 10^{-4}\ (\epsilon_\nu/10^{15}\ {\rm eV})^{0.5}$ is the probability that a neutrino produces a detectable high-energy muon for $\epsilon_\nu > 10^3$ TeV. We can see that the predicted neutrino number is well below the detection threshold of the most powerful neutrino detectors under construction. The main reason is that compared with GRBs, f_π (equation 27) is much smaller.

4 SUMMARY

We show that if a giant flare similar to the 2004 December 27 event occurs in the *GLAST* era, a strong sub-GeV flare shortly after the flare (originated from the hard tail of the synchrotron emission from the forward shock region) should be detectable if the outflow is relativistic. A positive/negative detection in the sub-GeV band would then give a diagnosis of the initial Lorentz factor of the outflow. With the available 10-MeV data (Mazets et al. 2005), we constrain $\Gamma_0 < 50$ for the December 27 event if the electron distribution is a single power law, although a higher Γ_0 is allowed if the electron distribution is a broken power law. At higher energies (e.g. above 1 GeV), a cut-off of the synchrotron emission is expected. Neither the SSC emission in the forward shock region nor the IC off the X-ray tail emission could give a detectable flux for *GLAST*.

The forward shock is able to accelerate protons to an energy $\sim 10^{17}$ eV. However, the time delay for these cosmic rays to reach us is very long, i.e. $\sim 10^6$ yr. Neutrinos with an energy 10^{14} eV are also predicted, but the flux is too low to be detected. Therefore, for a giant flare similar to the December 27 event taking place in the *GLAST* era, the most, and perhaps the only, interesting high-energy afterglow emission is the bright sub-GeV photon emission lasting for thousands of seconds.

ACKNOWLEDGMENTS

YZF thanks Drs Y. F. Huang and X. Y. Wang for helpful comments. This work is supported by NASA NNG04GD51G and a NASA Swift GI (Cycle 1) program (for BZ), the National Natural Science Foundation (grants 10225314 and 10233010) of China, and the National 973 Project on Fundamental Researches of China (NKBRSF G19990754; for DMW).

REFERENCES

Asano K., Yamazaki R., Sugiyama N., 2005, preprint (astro-ph/0503335)
Cameron P. B. et al., 2005, Nat, 434, 1112
Cheng K. S., Wang X. Y., 2003, ApJ, 593, L85
Corbel S., Eikenberry S. S., 2004, A&A, 419, 191
Dai Z. G., Wu X. F., Wang X. F., Huang Y. F., Zhang B., 2005, ApJ, submitted
Fan Y. Z., Zhang B., Wei D. M., 2005a, ApJ, in press (astro-ph/0412105)
Fan Y. Z., Zhang B., Wei D. M., 2005b, ApJ, in press (astro-ph/0504039)
Gaensler B. M. et al., 2005, Nat, 434, 1104
Gelfand J. D. et al., 2005, ApJ, submitted (astro-ph/0503269)
Granot J. et al., 2005, ApJ, submitted (astro-ph/0503251)
Halzen F., Landsman H., Montaruli T., 2005, preprint (astro-ph/0503348)
Huang Y. F., Dai Z. G., Lu T., 1998, Chin. Phys. Lett., 15, 775
Huang Y. F., Gou L. J., Dai Z. G., Lu T., 2000, ApJ, 543, 90
Hurley K. et al., 2005, Nat, 434, 1098
Ioka K., Razzaque S., Kobayashi S., Meszaros P., 2005, ApJL, submitted (astro-ph/0503279)
Krolik J. H., Pier E. A., 1991, ApJ, 373, 277

Mazets E. F., Cline T. L., Aptekar R. L., Frederiks D. D., Golenetskii S. V., Il'inskii V. N., Pal'shin V. D., 2005, preprint (astro-ph/0502541)
Nakar E., Piran T., Sari R., 2005, preprint (astro-ph/0502052)
Palmer D. A. et al., 2005, Nat, 434, 1107
Rybicki G. B., Lightman A. P., 1979, Radiative Processes in Astrophysics. Wiley, New York
Rhoads J. E., 1999, ApJ, 525, 737
Sari R., Esin A. A., 2001, ApJ, 548, 787
Thompson C., Duncan R. C., 2001, ApJ, 561, 980
Wang X. Y., Wu X. F., Fan Y. Z., Dai Z. G., Zhang B., 2005, ApJ, 623, L29
Yamazaki R., Ioka K., Takahara F., Shibazaki N., 2005, PASJ, in press (astro-ph/0502320)
Zhang B., Mészáros P., 2001, ApJ, 559, 110
Zhang B., Dai Z. G., Mészáros P., Waxman E., Harding A. K., 2003, ApJ, 595, 346

This paper has been typeset from a TEX/LATEX file prepared by the author.